The Journal of Immunology

Staphylococcus aureus Biofilms Prevent Macrophage Phagocytosis and Attenuate Inflammation In Vivo

Lance R. Thurlow, Mark L. Hanke, Teresa Fritz, Amanda Angle, Amy Aldrich, Stetson H. Williams, Ian L. Engebretsen, Kenneth W. Bayles, Alexander R. Horswill and Tammy Kielian

J Immunol 2011; 186:6585-6596; Prepublished online 27 April 2011;
doi: 10.4049/jimmunol.1002794
http://www.jimmunol.org/content/186/11/6585

The Journal of Immunology is published twice each month by
The American Association of Immunologists, Inc.,
1451 Rockville Pike, Suite 650, Rockville, MD 20852

Print ISSN: 0022-1767 Online ISSN: 1550-6606.

Staphylococcus aureus Biofilms Prevent Macrophage Phagocytosis and Attenuate Inflammation In Vivo

Lance R. Thurlow,*[,1] Mark L. Hanke,* Teresa Fritz,* Amanda Angle,* Amy Aldrich,* Stetson H. Williams,* Ian L. Engebretsen,[†] Kenneth W. Bayles,* Alexander R. Horswill,[‡] and Tammy Kielian*

Biofilms are complex communities of bacteria encased in a matrix composed primarily of polysaccharides, extracellular DNA, and protein. *Staphylococcus aureus* can form biofilm infections, which are often debilitating due to their chronicity and recalcitrance to antibiotic therapy. Currently, the immune mechanisms elicited during biofilm growth and their impact on bacterial clearance remain to be defined. We used a mouse model of catheter-associated biofilm infection to assess the functional importance of TLR2 and TLR9 in the host immune response during biofilm formation, because ligands for both receptors are present within the biofilm. Interestingly, neither TLR2 nor TLR9 impacted bacterial density or inflammatory mediator secretion during biofilm growth in vivo, suggesting that *S. aureus* biofilms circumvent these traditional bacterial recognition pathways. Several potential mechanisms were identified to account for biofilm evasion of innate immunity, including significant reductions in IL-1β, TNF-α, CXCL2, and CCL2 expression during biofilm infection compared with the wound healing response elicited by sterile catheters, limited macrophage invasion into biofilms in vivo, and a skewing of the immune response away from a microbicidal phenotype as evidenced by decreases in inducible NO synthase expression concomitant with robust arginase-1 induction. Coculture studies of macrophages with *S. aureus* biofilms in vitro revealed that macrophages successful at biofilm invasion displayed limited phagocytosis and gene expression patterns reminiscent of alternatively activated M2 macrophages. Collectively, these findings demonstrate that *S. aureus* biofilms are capable of attenuating traditional host proinflammatory responses, which may explain why biofilm infections persist in an immunocompetent host. *The Journal of Immunology*, 2011, 186: 6585–6596.

Biofilms are adherent communities of bacteria encased within a complex matrix that represents a considerable therapeutic challenge because organisms within these matrices are typically recalcitrant to conventional antibiotics. *Staphylococcus aureus* is capable of causing biofilm infections on both natural body surfaces including the lung and heart as well as medical devices such as indwelling catheters and prostheses (1–3). Further complicating this issue is the recent emergence of community-associated methicillin-resistant *S. aureus* (CA-MRSA) strains that are able to cause serious infections in otherwise healthy individuals (4, 5). Although the majority of CA-MRSA isolates have been recovered from skin and soft tissue infections, the ability of *S. aureus* to form biofilms presents a significant concern for the diagnosis and therapeutic treatment of these infections.

Although host immune responses to planktonic *S. aureus* have been extensively investigated (6–10), little information is currently available regarding host immunity to *S. aureus* biofilms or how the bacteria modulate antimicrobial effector mechanisms when organized in this protective milieu. Due to the communal nature of biofilms, bacteria within them may exhibit distinct properties compared with planktonic growth phases of the same species, which may lead to differences in how biofilms are recognized by the host immune response. To date, the majority of studies investigating the innate immune response to biofilms have been performed with *Pseudomonas aeruginosa* and *S. epidermidis*, in which neutrophils have been shown to phagocytize biofilm-associated bacteria and produce oxidative bursts, albeit at reduced levels compared with planktonic bacteria (11–16). To our knowledge, only a few reports exist in which leukocyte responses to *S. aureus* biofilm have been directly examined, most of which have been conducted in vitro (17–19). Therefore, additional mechanistic studies are needed to advance our understanding of the cross talk between *S. aureus* biofilm and host innate immunity.

Currently, the majority of studies investigating innate immunity to *S. aureus* have focused on neutrophils (20–22), whereas macrophage responses to staphylococcal species have received relatively less attention. Although neutrophils are important antimicrobial effectors, their transcriptional capacity for inflammatory cytokine/chemokine production is limited, and their short lifespan requires constant neutrophil recruitment due to cell turnover. In comparison, macrophages are more long-lived, produce high levels of proinflammatory mediators upon bacterial exposure that are critical for amplifying immune cell recruitment/activation cascades, and also

*Department of Pathology and Microbiology, University of Nebraska Medical Center, Omaha, NE 68198; [†]Department of Biology, Wayne State College, Wayne, NE 68787; and [‡]Department of Microbiology, Carver College of Medicine, University of Iowa, Iowa City, IA 52242

[1]Current address: Department of Microbiology and Immunology, University of North Carolina at Chapel Hill Medical School, Chapel Hill, NC.

Received for publication August 18, 2010. Accepted for publication April 3, 2011.

This work was supported by the National Institutes of Health National Institute of Allergy and Infectious Diseases P01 AI083211 Project 4 (to T.K.) and Project 3 (to A.R.H.).

Address correspondence and reprint requests to Dr. Tammy Kielian, Department of Pathology and Microbiology, University of Nebraska Medical Center, 985900 Nebraska Medical Center, Omaha, NE 68198-5900. E-mail address: tkielian@unmc.edu

The online version of this article contains supplemental material.

Abbreviations used in this article: 7-AAD, 7-aminoactinomycin D; BMDM, bone marrow-derived macrophage; CA-MRSA, community-associated methicillin-resistant *S. aureus*; CTO, CellTracker Orange; eDNA, extracellular DNA; erm, erythromycin resistance; iNOS, inducible NO synthase; IVIS, In Vivo Imaging System; KO, knockout; PGN, peptidoglycan; PIA, polysaccharide intercellular adhesion; PRR, pattern recognition receptor; qRT-PCR, quantitative real-time RT-PCR; SEM, scanning electron microscopy; Tg, transgenic; TSB, trypticase soy broth; UNMC, University of Nebraska Medical Center; WT, wild-type.

exhibit potent phagocytic and antimicrobial effects (23, 24). In addition, resident macrophages are present in virtually all tissues and serve as a critical first line of defense against microbial invasion, in part, via bacterial recognition via TLRs, which are discussed below. Therefore, macrophages represent another critical antimicrobial effector population; however, their responses to *S. aureus* biofilms remain to be defined.

Previous studies have demonstrated that bacterial biofilms, including those formed by *S. aureus*, are encased in a complex matrix composed of polysaccharides, extracellular DNA (eDNA), and proteins (25–28). It is well known that these microbial structural motifs are recognized by the innate immune system, in part, via the TLR family of pattern recognition receptors (PRRs). Upon activation, TLR signaling leads to the secretion of numerous proinflammatory mediators that serve to recruit and activate additional immune cell populations to sites of infection (29–35). TLR2 mediates recognition of several pathogen-associated molecular patterns expressed by *S. aureus* that are released during normal bacterial growth and lysis (36–39) including lipoproteins, peptidoglycan (PGN), and lipoteichoic acids (40–42). Numerous cell types express TLR2 including macrophages, dendritic cells, and neutrophils, and recent reports have revealed that phagocytosis of *S. aureus* is required to trigger TLR2-dependent signaling within the phagosome and inflammasome activation (43, 44). TLR9 is an intracellular receptor that recognizes unmethylated CpG motifs characteristic of bacterial DNA (31, 45). Upon phagocytosis and digestion of *S. aureus* in the phagosome, bacterial DNA is liberated and engages TLR9. However, eDNA can also trigger TLR9-dependent activation, which is relevant to biofilms due to the extensive amount of eDNA contained in the matrix (2, 25, 28). Although several studies have demonstrated that both TLRs are pivotal for host immune responses to planktonic *S. aureus* and associated pathogen-associated molecular patterns (7, 46, 47), to our knowledge, the role of TLR2 and TLR9 in regulating host immunity to biofilm growth has not yet been examined in response to biofilm formed by any bacterial species.

Using a mouse model of catheter-associated biofilm infection, we demonstrate for the first time, to our knowledge, that *S. aureus* biofilms actively attenuate traditional antibacterial immune responses, as demonstrated by significant reductions in cytokine/chemokine production associated with biofilm-infected tissues compared with the wound healing response elicited by sterile catheters. In agreement with this apparent immune deviation, a role for either TLR2 or TLR9 in regulating biofilm infection in vivo could not be demonstrated. Several mechanisms were identified that could account for the persistence of biofilm infection including minimal inducible NO synthase (iNOS) induction concomitant with robust arginase-1 expression at the host–biofilm interface. In addition, although macrophage infiltration into biofilm infections was prominent, immunofluorescence staining revealed that few cells were able to migrate into the biofilm. Finally, biofilms induced significant and rapid cell death in those macrophages that invaded deep into the biofilm and programmed macrophages toward an alternatively activated M2 phenotype, suggesting additional mechanisms of immune deviation. Collectively, these studies demonstrate the unique properties of *S. aureus* biofilms to circumvent traditional antimicrobial effector pathways and persist in an immunocompetent host.

Materials and Methods

Mouse strains

TLR2 and TLR9 knockout (KO) mice (generously provided by Dr. Shizuo Akira, Osaka University, Osaka, Japan) have been backcrossed with C57BL/6 mice for a total of eight generations, and C57BL/6 mice (Charles River Laboratories, Frederick, MD) were used as wild-type (WT) controls. Bone marrow-derived macrophages (BMDM) were generated from GFP transgenic (Tg) mice (C57BL/6-Tg[CAG-EGFP]) (The Jackson Laboratory, Bar Harbor, ME). The animal use protocol, approved by the University of Nebraska Medical Center (UNMC) Animal Care and Use Committee, is in accord with the National Institutes of Health guidelines for the use of rodents.

S. aureus *strains*

S. aureus strain USA300 LAC was obtained from Dr. Frank DeLeo (National Institute of Allergy and Infectious Diseases Rocky Mountain Laboratories, Hamilton, MT) (48, 49). For in vivo imaging studies, USA300 LAC chromosomally transduced with the bacterial luciferase gene *lux* was used (Xen 29; Caliper Life Sciences, Hopkinton, MA; USA300 LAC::*lux*).

In vivo model of S. aureus *biofilm infection*

The impact of TLR2 or TLR9 on biofilm formation and growth in vivo was assessed using a mouse model of catheter-associated biofilm infection as previously described with minor modifications (50, 51). Briefly, WT, TLR2 KO, or TLR9 KO mice received s.c. implants of sterile 1-cm catheter segments in both flanks under general anesthesia. One catheter was inoculated with 20 μl (5×10^5 CFU) log-phase USA300 LAC::*lux*, whereas the other catheter received an equal volume of PBS to evaluate the foreign body response. The extent of biofilm formation was monitored longitudinally in the same cohort of mice using an In Vivo Imaging System (IVIS Spectrum; Caliper Life Sciences) under isoflurane anesthesia, and separate groups of animals were sacrificed at days 3, 7, and 10 postinfection to determine absolute bacterial burdens associated with catheters and surrounding tissues. In experiments designed to assess the ability of identical *S. aureus* inoculums to establish biofilm versus s.c. infection in the absence of an indwelling device, mice received s.c. injections of USA300 LAC::*lux* (5×10^5 CFU in 20 μl) and processed as described above for biofilm infections.

Scanning electron microscopy

Catheters and associated tissues were harvested from mice at day 10 postinfection and fixed with 0.1 M Sorensen's phosphate buffer containing 2% glutaraldehyde and 2% paraformaldehyde. Fixed specimens were cut longitudinally and washed three times in 0.1 M Sorensen's phosphate buffer. The specimens were dehydrated using a graded series of ethanol washes and critical pointed dried in a Pelco CPD2 critical point dryer (Ted Pella, Redding, CA). Dried specimens were mounted on aluminum stubs with carbon tabs and colloidal silver paste and sputter coated with gold-palladium using a Hummer VI sputter coater (Anatech, Battle Creek, MI). Samples were viewed using a Quanta 200 scanning electron microscope (FEI, Hillsboro, OR) operated at 25 kV.

Flow cytometry

To compare the degree of macrophage influx into *S. aureus* biofilms versus s.c. abscesses, FACS analysis was performed. Briefly, abscesses and catheter-associated tissues were collected at days 3, 7, and 14 postinfection and minced in HBSS supplemented with 10% FBS (HyClone, Logan, UT) and filtered through a 70-μm nylon mesh cell strainer. The resulting slurry was digested for 30 min at 37°C in HBSS supplemented with 2 mg/ml collagenase type I and 28 U/ml DNAse I (both from Sigma-Aldrich, St. Louis, MO) to obtain a single-cell suspension. Following enzyme neutralization, cells were layered onto a discontinuous Percoll gradient (1.03–1.088 g/ml) and centrifuged at 2400 rpm for 20 min at room temperature in a swinging bucket rotor, whereupon the cell interface was collected. Following extensive washes and incubation in Fc Block (BD Biosciences, San Diego, CA) to minimize nonspecific Ab binding to Fc receptors, cells were stained with F4/80-FITC (AbD Serotec, Raleigh, NC) to identify macrophages. Cells were analyzed using a BD FACSAria (BD Biosciences) with compensation set based on the staining of each individual fluorochrome alone and correction for autofluorescence with unstained cells. Controls included cells incubated with isotype control Abs to assess the degree of nonspecific staining.

Immunofluorescence staining and confocal microscopy

Biofilm-associated and abscess tissues were collected at days 7 and 14 following infection, fixed in 10% formalin, and embedded in paraffin, whereupon paraffin sections (10 μm) were prepared by the UNMC Tissue Science Facility for H&E, Gram, and immunofluorescence staining. Sections were deparaffinized in xylene, and a graded series of alcohols and Ag

retrieval was performed by microwaving sections in 10 mM NaCi buffer (pH 6) for 14 min. Next, tissues were rinsed once in 1× PBS (pH 7.4) and stained with Abs specific for arginase-1 (Santa Cruz Biotechnology, San Diego, CA), iNOS (Abcam, Cambridge, MA), and Iba-1 (macrophage-specific marker; Biocare Medical, Concord, CA). Staining was detected using either FITC-conjugated or biotinylated secondary Abs (obtained from Jackson ImmunoResearch Laboratories, West Grove, PA), the latter of which was followed by a streptavidin-594 conjugate (Invitrogen). Confocal images were acquired using a Zeiss 510 META laser scanning confocal microscope (Carl Zeiss, Thornwood, NY), and staining specificity was confirmed by the absence of fluorescence signal following incubation of tissues with secondary Abs alone.

Gentamicin protection assays

To determine whether macrophages recovered from biofilm-infected tissues harbored viable *S. aureus* intracellularly, gentamicin protection assays were performed at day 7 postinfection as previously described (52). Day 7 was the only interval examined, as this represented the time point at which maximal catheter colonization had occurred. Following macrophage recovery by FACS, an aliquot of cells was taken to determine total bacterial counts (extra- and intracellular organisms). A second aliquot of sorted macrophages was exposed to 100 μg/ml gentamicin for 2 h at 37˚C to kill extracellular organisms, whereupon macrophages were washed twice to remove residual gentamicin, lysed using sterile distilled water, and intracellular bacterial titers enumerated. To ensure that intracellular bacteria were sensitive to an antibiotic that can penetrate mammalian cell membranes, macrophages were incubated with 1 mg/ml rifampicin. Results are expressed as the number of viable intracellular *S. aureus* per 10^3 biofilm-associated macrophages.

ELISA

To compare the production of inflammatory mediators associated with biofilm-infected versus sterile catheters of WT, TLR2 KO, and TLR9 KO mice, sandwich ELISA kits were used to quantitate TNF-α, IL-1β, and CCL2 (OptiEIA; BD Biosciences) or CXCL2 (DuoSet; R&D Systems) levels. Results were normalized to the amount of total protein recovered to correct for differences in tissue sampling size.

Generation of S. aureus *static biofilms in vitro*

The USA300 LAC strain was cured of its plasmid encoding erythromycin resistance (erm) to facilitate genetic manipulation. The erm-sensitive variant was transformed with plasmid pCM11 to express GFP driven by the *sarA* P1 promoter (USA300 LAC-GFP), and plasmid expression was maintained with erm selection (10 μg/ml) (53). Our initial investigation of macrophage–*S. aureus* biofilm interactions used trypticase soy broth (TSB). Although this broth formulation was compatible with biofilm growth, it induced changes characteristic of apoptosis in macrophages (data not shown). Therefore, we evaluated the growth kinetics of USA300 LAC-GFP in defined macrophage medium (i.e., RPMI 1640 supplemented with 10% heat-inactivated FBS) compared with TSB. Biofilm maturation was slightly delayed in macrophage medium compared with equivalent growth periods in TSB, and biofilms propagated for either 4 or 6 d were selected for further analysis based on their differing degrees of structural maturity. Specifically, 4-d-old biofilms were considered more immature in terms of average thickness (34 μm) and irregular density, whereas 6-d-old biofilms were classified as mature based on a relatively uniform thickness (52 μm average), presence of tower structures, and more consistent density (Supplemental Fig. 1). Biofilms were stained with TOTO3 or WGA-Alexa Fluor 633 (both from Molecular Probes, San Diego, CA) to visualize eDNA/dead cells or polysaccharide intercellular adhesion (PIA), respectively. TOTO3 staining revealed some eDNA/dead bacteria at the biofilm base with additional staining located throughout the structure in a punctate staining pattern (Supplemental Fig. 1 and data not shown). Both 4- and 6-d-old biofilms also expressed PIA as assessed by WGA staining (data not shown).

To generate static biofilms, sterile two-well glass chamber slides (Nunc, Rochester, NY) were treated with 20% human plasma (kindly provided by Dr. Steve Carson, UNMC) in sterile carbonate-bicarbonate buffer (Sigma-Aldrich) overnight at 4˚C to facilitate bacterial attachment (50). Starter cultures of USA300 LAC-GFP were prepared from a single bacterial colony and incubated overnight in macrophage medium supplemented with 10 μg/ml erm at 37˚C while shaking at 250 rpm under aerobic conditions. The following day, plasma coating buffer was removed and each chamber inoculated with USA300 LAC-GFP (diluted to an OD_{600} of 0.050; 2 ml/chamber), whereupon bacteria were incubated at 37˚C under static aerobic conditions for a period of up to 6 d. Medium was carefully replenished every 24 h to prevent disruption of the biofilm structure.

Preparation of bone marrow-derived and thioglycollate-elicited peritoneal macrophages

C57BL/6 mice were used to procure thioglycollate-elicited peritoneal macrophages as previously described (54). Elicited macrophages were washed extensively and labeled with 5 μM CellTracker Orange (CTO; Molecular Probes) for visualization according to the manufacturer's instructions. Macrophage cell counts and viability following CTO staining were determined using trypan blue dye exclusion. Initial optimization experiments verified that CTO labeling did not affect macrophage proinflammatory responses to planktonic *S. aureus* or cell viability (data not shown). For experiments to examine the impact of *S. aureus* biofilms on macrophage gene expression, BMDM were prepared from GFP Tg mice by flushing long bones with sterile 1× PBS and culturing cells in macrophage medium supplemented with 10 μg/ml M-CSF (Invitrogen). FACS analysis verified that >95% of cells were macrophages based on F4/80 staining (data not shown).

Macrophage-biofilm coculture models

CTO-labeled macrophages were added to biofilms at 10^7 cells/chamber prior to observation by confocal microscopy. Based on enumeration of bacterial densities within the biofilm, this equated to a multiplicity of infection of 10:1 (bacteria/macrophage). Slides were incubated with macrophages at 37˚C under static aerobic conditions for either 1 or 24 h prior to observation. To determine how macrophage interactions may vary during biofilm versus planktonic growth, macrophages were also incubated with planktonic bacteria in identical glass chamber slides that had not been precoated with human plasma. In some experiments, TOTO3 staining was performed to discriminate between viable versus dead macrophages, which could be differentiated from dead bacteria based on size. Macrophage–biofilm or –planktonic interactions were visualized at the appropriate time point using a Zeiss laser scanning confocal microscope (LSM 510 META; Carl Zeiss). The confocal pinhole was set to obtain an optical section thickness of 1 μm. Z-stacks (100–150 μm in thickness) were collected from beneath the glass slide extending to above the point where CTO-labeled macrophages could be detected. Three-dimensional images of biofilms and measurements to demonstrate the relative proximity of macrophages from the biofilm surface were made using Xen 2007 software (Carl Zeiss). All confocal image files were subjected to a coding strategy to ensure that the observer performing quantitations was blinded to treatment group identity to avoid potential bias during analysis.

The impact of *S. aureus* biofilms on macrophage activation was evaluated by quantitative real-time RT-PCR (qRT-PCR). Briefly, GFP^+ BMDM were incubated with USA300 LAC static biofilms for 2 h as described above or planktonic bacteria for comparison, followed by mechanical dissociation by trituration. Subsequently, both preparations were incubated with the vital dye 7-aminoactinomycin D (7-AAD; eBioscience, San Diego, CA), and viable macrophages (GFP^+, $7\text{-}AAD^-$) were collected by FACS. Total RNA was isolated from sorted macrophages using a TaqMan Pre-Amp Cells-to-Ct kit (Applied Biosystems, San Diego, CA) for limiting cell numbers and qRT-PCR performed for iNOS, arginase-1, TNF-α, and IL-1β. Results were normalized against cycle thresholds for the housekeeping gene GAPDH and are presented as the fold-change ($2^{-\Delta\Delta Ct}$) of macrophages exposed to biofilms relative to planktonic bacteria (mean ± SEM from four independent experiments).

Phagocytosis assay

To determine whether macrophages were capable of phagocytizing disrupted biofilm material, *S. aureus* biofilms were mechanically triturated and fragments incubated with macrophages for phagocytosis assays as previously described (55–57). Macrophages were exposed to planktonic bacteria at a 1:10 ratio as a control. Samples were incubated at 37˚C for 30 min to allow bacterial uptake by macrophages, whereupon trypsin was added at a final concentration of 0.25% for 10 min to remove any residual bacteria at the macrophage surface. Macrophages were washed 3× with PBS to remove remaining bacteria, fixed to glass slides by cytocentrifugation (CytoSpin; Thermo Scientific), and viewed under 40× oil immersion using a Zeiss Observer A.1 fluorescent microscope (Carl Zeiss) to evaluate the presence of intracellular GFP^+ bacteria.

Statistics

Significant differences in bacterial titers and cytokine expression between experimental groups were determined using the Student *t* test with Welch's correction for unequal variances, and FACS data were evaluated by one-way ANOVA followed by the Holm-Sidak method for multiple pairwise comparisons. For all analyses, a p value <0.05 was considered statistically significant.

Results

Establishment of S. aureus *biofilms in vivo*

Because bacterial biofilms are typically associated with chronic indolent infections, they are presumed to evade the host immune response, yet few studies to date have provided scientific evidence to substantiate this phenomenon in vivo, which was the primary objective of this work. We used a mouse model in which biofilms were established on surgically implanted catheters, which mimics biofilm formation associated with infected medical devices in humans (50, 51). Evaluation of tissues surrounding infected catheters by Gram-staining revealed evidence of biofilm growth within the catheter lumen as well as the catheter-tissue interface (Fig. 1*A*, 1*B*, respectively). At the ultrastructural level, scanning electron microscopy (SEM) also verified biofilm formation at the interface of the catheter and surrounding host tissue (Fig. 1*C*). Interestingly, based on size differentials, it was apparent that host cells were not capable of forming intimate associations with the biofilm (Fig. 1*C*, arrows). Detailed examination of the catheter lumen by SEM revealed a contiguous bacterial layer with the appearance of tower structures (Fig. 2*A*, 2*B*). The interior of these towers was largely hollow, and higher magnification revealed the presence of an extensive fiber network, presumably matrix material that aggregated during the SEM dehydration process (Fig. 2*C*). These structural features are reminiscent of the tower structures observed during in vitro biofilm growth conditions (28, 58). Collectively, these findings demonstrate the formation of a bona fide *S. aureus* biofilm in vivo, allowing an assessment of the importance of innate immunity in regulating the host response to biofilm infection.

S. aureus *biofilms evade TLR2 and TLR9 recognition in vivo*

Because both TLR2 and TLR9 ligands are present within *S. aureus* biofilms (i.e., lipoproteins/PGN and eDNA, respectively), we next examined what functional role these receptors play in enabling biofilm recognition utilizing TLR2 and TLR9 KO mice. For these studies, we compared the establishment of catheter-associated biofilm formation versus abscesses induced by the s.c. inoculation of *S. aureus* in the absence of an indwelling device. The rationale for this approach was 2-fold: first, it allowed us to evaluate whether TLR2 or TLR9 exert differential roles in bacterial clearance between biofilm versus s.c. infections; and second, it enabled an assessment of the importance of an indwelling device for bacterial persistence. Surprisingly, in vivo imaging studies and bacterial enumeration revealed that the degree of biofilm infection was qualitatively (Fig. 3) and quantitatively (Fig. 4) similar between TLR2 and TLR9 KO mice compared with WT animals. In addition, by comparing the ability of identical *S. aureus* inoculums to develop biofilm versus s.c. infection, we demonstrated an essential role for an indwelling catheter in establishing sustained infection. Specifically, prominent bioluminescent signals and bacterial burdens were detected in biofilm infected WT, TLR2 KO, and TLR9 KO mice, whereas minimal bacterial growth was detected in animals inoculated with *S. aureus* in the absence of an indwelling catheter (Figs. 3, 4). Although previous studies have demonstrated that TLR2 and TLR9 are important for bacterial containment in other models of bloodstream or s.c. infection, these studies required extremely high bacterial inoculums to show any phenotypes (7, 35). In contrast, our experiments used a relatively low infectious dose (i.e., 5×10^5 CFU), which was rapidly cleared and implicates the involvement of alternative PRRs. Collectively, these findings highlight the ability of *S. aureus* to persist in the context of an indwelling device and circumvent recognition by traditional PRRs that would normally be triggered by planktonic bacteria. This speaks to the immune evasiveness of biofilms that is evident from a clinical perspective.

S. aureus *biofilms actively attenuate host proinflammatory responses*

We next evaluated whether *S. aureus* biofilms would alter proinflammatory mediator secretion profiles in an attempt to explain why these infections persist in an immunocompetent host. Examination of several inflammatory signals responsible for macrophage and neutrophil recruitment (CCL2 and CXCL2, respectively) and activation (TNF-α and IL-1β) were significantly attenuated in biofilm-infected tissues compared with the wound healing response elicited following the insertion of sterile catheters (Fig. 5). Again, no differences in inflammatory mediator expression were observed between biofilm-infected tissues from WT, TLR2 KO, or TLR9 KO mice (data not shown), which correlated with the failure to detect significant differences in bacterial burdens in these animals (Supplemental Figs. 2, 3).

To further investigate mechanisms of immune deviation associated with biofilm infections, we compared the degree of macrophage influx into *S. aureus*-induced abscesses versus catheter-associated biofilms by FACS. Interestingly, macrophage accumulation into biofilm-infected tissues was significantly increased at day 3 postinfection compared with abscesses (Fig. 6). Despite this early exaggerated macrophage infiltrate, immunofluorescence staining demonstrated that the majority of cells remained distant from the infection site, with only a few macrophages recruited to the biofilm surface (Fig. 7). Collectively, these findings demonstrate that *S. aureus* biofilms evade traditional TLR recognition and alter the immune response to infection.

Biofilm infections attenuate iNOS and augment arginase-1 expression in vivo

Reactive nitrogen intermediates represent a major microbicidal mechanism and are synthesized in macrophages by iNOS (59). In

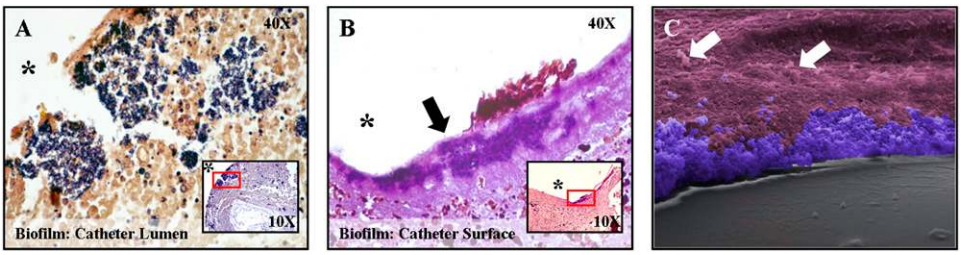

FIGURE 1. Characterization of *S. aureus* localization during biofilm development. Catheters and surrounding tissues were isolated from WT mice at day 10 following *S. aureus* infection and subjected to Gram-staining (*A*, *B*) or SEM (*C*). There was evidence of bacterial growth (purple) within the catheter lumen (*A*) as well as host tissue immediately surrounding the catheter (*B*, arrow). *Insets* in *A* and *B* depict original magnification ×10 with red rectangles indicating the area enlarged at original magnification ×40 and asterisks denoting the original location of infected catheters that were nonadherent to glass slides. Original magnification ×400 SEM image (*C*) has been pseudocolored to highlight *S. aureus* biofilm (blue) at the interface between the catheter (gray) and surrounding host tissue (purple). Host cells located at a distance from the biofilm are indicated by arrows.

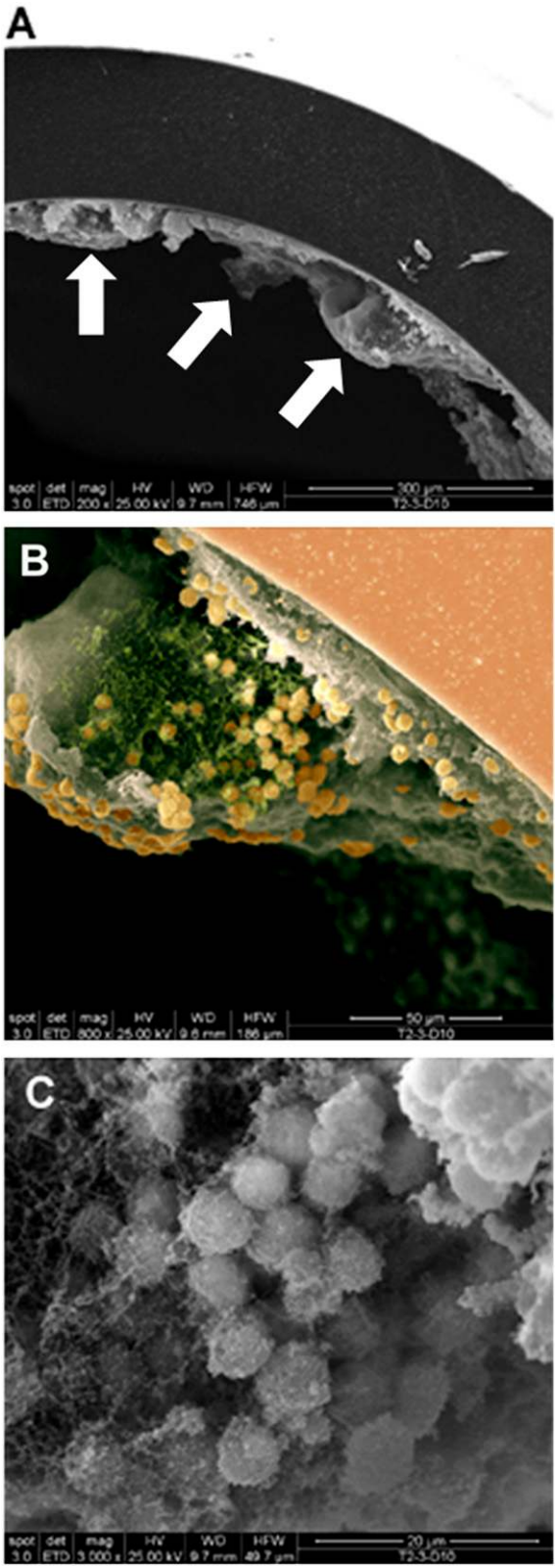

FIGURE 2. Evidence of catheter-associated biofilm growth in vivo. Catheters were isolated from WT mice at day 10 following *S. aureus* infection and processed for SEM analysis. The smooth surface at the periphery of the images in *A* and *B* represents the catheter with biofilm visible on the internal face. *A*, Original magnification ×200 demonstrating the irregular undulating pattern of the biofilm surface (arrows indicate tower structures). *B*, Higher magnification of a tower from the image shown in *A* revealing a predominantly hollow interior with numerous cocci at the margins (original magnification ×800). The image has been pseudocolored to highlight *S. aureus* (gold) and presumably matrix material (green), which likely aggregated during the SEM dehydration process, from the remaining biofilm structure (gray; original magnification ×800). The smooth surface at the upper right represents the catheter (salmon) with biofilm visible on the internal face. *C*, Original magnification ×3000 of an *S. aureus* cluster within the tower depicted in *B*.

contrast, arginase-1 leads to L-proline production, which is a precursor in the collagen biosynthetic pathway (60, 61). Both iNOS and arginase-1 compete for the same substrate (arginine) and, as such, are differentially expressed (62). Due to the fact that biofilm infections are typically associated with a fibrotic response and because of their chronic nature, we investigated whether differences in iNOS and arginase-1 expression would be evident. Indeed, iNOS expression associated with biofilm infections was reduced compared with abscesses and coincided with robust arginase-1 expression (Fig. 8). In addition, arginase-1 expression was detected in macrophages in closest proximity to the biofilm, although other cell type(s) were also arginase positive (Fig. 9). Arginase-1 expression in biofilm-associated macrophages in the absence of iNOS would be expected to skew the cellular response away from bacterial killing and could be another mechanism to account for the ability of biofilms to evade clearance.

Biofilms program macrophages toward an alternatively activated M2 phenotype

Our in vivo studies had clearly demonstrated that *S. aureus* biofilms were capable of circumventing traditional antibacterial effector mechanisms. To further examine potential mechanisms responsible for this phenomenon and to simplify the study of biofilm–macrophage interactions without confounds from other cell types, we next explored the effects of *S. aureus* biofilms on macrophage responses in vitro.

To date, few studies have examined the interactions between *S. aureus* biofilm and macrophages, which are an important antibacterial effector population. To determine whether biofilms influence macrophage activation, gene expression profiles were compared between macrophages incubated with either *S. aureus* biofilms or planktonic bacteria. Similar to our in vivo findings, macrophages cocultured with biofilms demonstrated a gene expression profile reminiscent of alternatively activated M2 cells, namely a reduction in iNOS coincident with a significant increase in arginase-1 expression, whereas no differences in TNF-α or IL-1β were observed (Fig. 10) (63). These results further support the conclusion that biofilm growth reprograms the macrophage response from a bactericidal M1 to an M2 phenotype, the latter of which is not optimal for maximal bacterial clearance (63, 64).

Macrophages actively phagocytize planktonic S. aureus *but not biofilm-associated bacteria in vitro*

Previous studies have suggested that neutrophils are capable of phagocytizing *S. aureus* biofilms (18, 19); however, less is known about the ability of macrophages to internalize bacteria in a biofilm state. To this end, we incubated primary mouse peritoneal macrophages with either 4- or 6-d-old *S. aureus* static biofilms and evaluated their phagocytic ability. Interestingly, macrophages incubated with *S. aureus* biofilms for either a 1- or 24-h period contained few internalized bacteria (Fig. 11*A* and data not shown). Similar findings were also obtained with BMDM (data not shown). In contrast to macrophages, intracellular bacteria were readily discernable in neutrophils cocultured with either 4- or 6-d-old biofilms (Supplemental Fig. 4), demonstrating the sensitivity of confocal analysis for visualizing intracellular organisms. The

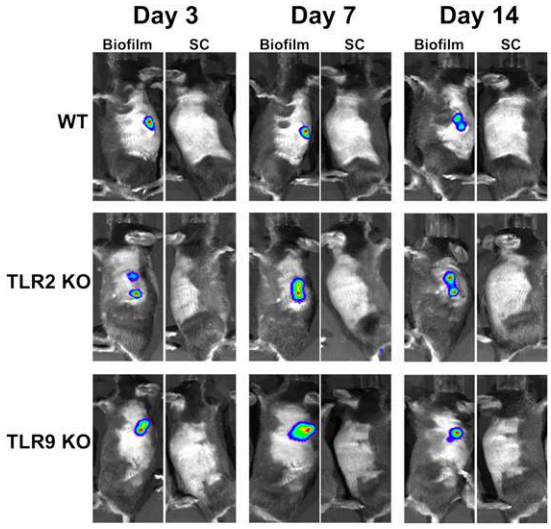

FIGURE 3. Visualization of *S. aureus* biofilm infection using IVIS. WT, TLR2 KO, and TLR9 KO mice were infected with 5×10^5 CFU USA300 LAC::*lux* either in the lumen of surgically implanted catheters to establish biofilm infection or s.c. in the absence of any indwelling device. At the indicated time points postinfection, mice were subjected to IVIS imaging to visualize the extent of biofilm or s.c. infection. Images are presented from one mouse per group that was imaged at all time points to map the progression of biofilm infection.

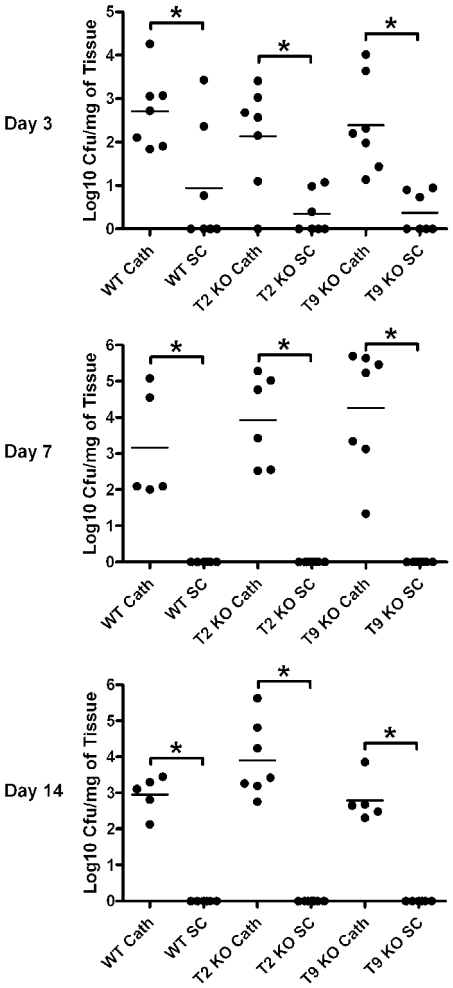

FIGURE 4. Infection with an equivalent *S. aureus* dose leads to the establishment of catheter-related biofilm infection but rapid clearance from s.c. sites. WT, TLR2 KO, and TLR9 KO mice were infected with 5×10^5 CFU USA300 LAC::*lux* either in the lumen of surgically implanted catheters (Cath) to establish biofilm infection or s.c. (SC) in the absence of any indwelling device. Animals were sacrificed at the indicated days following *S. aureus* infection, whereupon host tissues surrounding infected catheters or s.c. injection sites were homogenized to quantitate bacterial burdens. Results are expressed as the number of CFU per mg host tissue to correct for differences in tissue sampling size. Significant differences in bacterial burdens between biofilm-infected versus s.c. injected mice are denoted by asterisks. *$p < 0.001$.

impact of *S. aureus* biofilms on neutrophil function will be the topic of a separate manuscript (M. L. Hanke and T. Kielian, manuscript in preparation). The inability of macrophages to phagocytize biofilm-associated bacteria was independent of the age of the biofilm in that intracellular bacteria could not be observed in macrophages incubated with either 4- or 6-d-old biofilms (Fig. 11*A* and data not shown). In addition, macrophages did not significantly impact the number of biofilm-associated bacteria during the 24-h coincubation period (data not shown). These findings indicate that although macrophages are capable of infiltrating biofilms, phagocytic mechanisms are not discernable during this growth state. However, macrophages were capable of internalizing disrupted biofilm material (Fig. 11*B*), suggesting that the size and/or physical complexity of the intact biofilm are responsible for its inability to be phagocytized. As expected, macrophages were highly phagocytic toward planktonic *S. aureus* (Fig. 11*A*), indicating that they were capable of recognizing bacteria in this growth state.

In contrast to these in vitro studies, macrophages recovered from biofilm infections in vivo harbored intracellular *S. aureus* as demonstrated by gentamicin protection assays (Fig. 12). The intracellular location of bacteria was confirmed by the ability of rifampicin, which is capable of crossing the eukaryotic cell membrane, to completely eliminate viable organisms (Fig. 12). However, this approach cannot discriminate between uptake of biofilm-associated versus planktonic bacteria, the latter of which occurs during biofilm dispersal in an attempt to colonize new sites of infection (28, 65, 66). Collectively, the fact that a large percentage of macrophages remain significantly distant from the biofilm surface in conjunction with reduced iNOS expression suggests that even though macrophages exhibit a modest degree of phagocytosis, intracellular killing mechanisms are likely compromised.

Macrophage invasion into biofilms in vitro is associated with cell death

Based on the ineffectiveness of the host immune response to clear *S. aureus* biofilms in vivo, it is likely that the biofilm compromises numerous antibacterial effector mechanisms to persist in the host. To further investigate such possibilities, we next examined whether biofilms adversely affected macrophage survival. Interestingly, a striking difference in cell morphology was observed between macrophages incubated with 4- versus 6-d-old biofilms for a 24-h period. Namely, macrophages exposed to immature biofilms (i.e., 4-d-old) exhibited a typical rounded morphology, whereas macrophages incubated with mature biofilms (i.e., 6-d-old) appeared ghostlike with a dystrophic morphology as evidenced by their irregular shape and diminished CTO staining (Fig. 13). Because a mature (i.e., 6-d-old) biofilm represents a dense matrix network composed of polysaccharides, eDNA, and protein polymers, it is likely that this presents the macrophage with a substrate that is difficult to phagocytize, resulting in a phenomenon termed frustrated phagocytosis (67). Although macrophages exposed to immature biofilms retained a typical cell appearance, TOTO3 staining revealed that those macrophages most intimately associated with the biofilm were dead, whereas the majority of

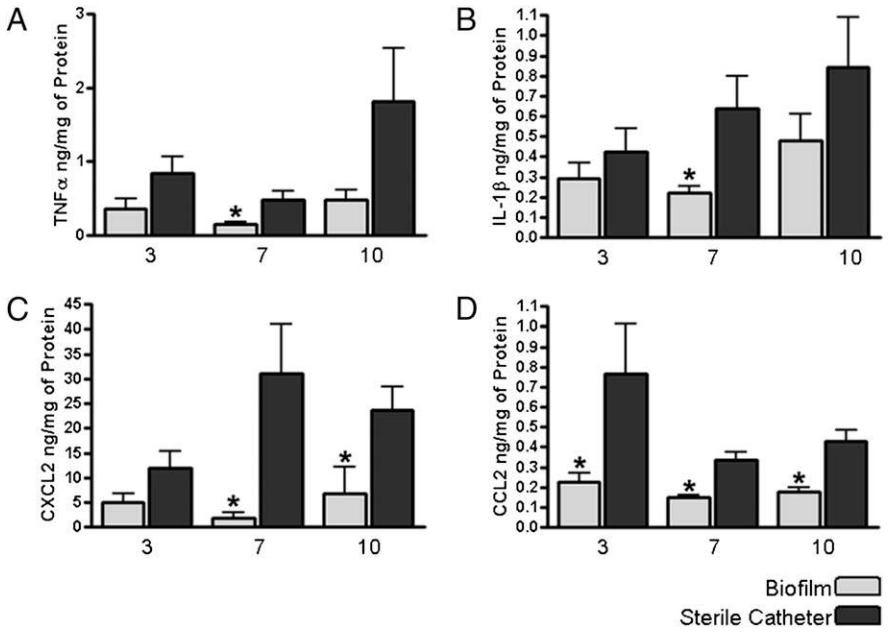

FIGURE 5. *S. aureus* biofilms attenuate inflammatory mediator expression compared with the wound healing response elicited following sterile catheter implantation. Tissues surrounding *S. aureus* infected or sterile catheters from WT mice were collected and homogenized at the indicated time points to obtain supernatants to quantitate differences in TNF-α (*A*), IL-1β (*B*), CXCL2 (*C*), or CCL2 (*D*) expression by ELISA. Results were normalized to the amount of total protein recovered to correct for differences in tissue sampling size. Significant differences in inflammatory mediator expression between biofilm-infected versus sterile catheters are denoted by asterisks. Results are presented from individual animals combined from three independent experiments. $*p < 0.05$.

macrophages farther removed from the biofilm surface remained viable (Fig. 14). This live/dead cell analysis could not be conducted on macrophages incubated with 6-d-old biofilms due to the ghostlike dystrophic nature of the cells. Similar cell death patterns were observed during FACS studies with the vital dye 7-AAD, in which ~55% of macrophages were dead within 2 h following biofilm coculture (data not shown). The mechanisms responsible for this rapid induction of cell death are not known but may be influenced by toxin production, acidic pH, and/or anaerobic conditions within the biofilm proper. Collectively, these studies reveal that *S. aureus* biofilms induce macrophage dysfunction and cell death, which could contribute to biofilm evasion of host immunity and persistence in vivo (Fig. 15).

Discussion

To date, relatively little information is available regarding how innate immunity interfaces with *S. aureus* biofilms. Because *S. aureus* biofilms represent a serious clinical situation based on their recalcitrance to antibiotics, persistence, and the propensity of organisms to detach and colonize new infection sites (68, 69), understanding the dynamics between host immunity and *S. aureus* biofilms is an important issue that warrants further investigation.

To our knowledge, this study is the first to report that *S. aureus* biofilms actively modify the host innate immune response in vivo by attenuating proinflammatory cytokine production and circumventing traditional bacterial recognition pathways mediated by TLR2 and TLR9. In addition, iNOS levels were significantly reduced surrounding biofilm infections and instead were dominated by arginase-1 expression. In the context of biofilm infection, the skewing from iNOS to an arginase-1 prominent response is likely another explanation for why biofilm infections persist in an immunocompetent host. The innate immune alterations associated with biofilm infection identified in this study are summarized in Fig. 15.

The rationale for our investigation of TLR2 and TLR9 stemmed from the fact that their ligands are components of the biofilm (25–28). Although TLR2 has been shown to play a pivotal role in *S. aureus* recognition and clearance in several in vivo models of planktonic infection, it is clear that when *S. aureus* assumes a biofilm lifestyle, the organism is capable of evading recognition by this classical PRR. This finding highlights the importance of bacterial growth state in dictating whether innate immune sensor mechanisms will be effective at clearing the infection. It was also unexpected that we did not observe a dramatic role for TLR9 in regulating biofilm growth since a recent report demonstrated that eDNA was a major proinflammatory stimulus of *P. aeruginosa* biofilms (70). However, this discrepancy may be attributed to several factors including making comparisons between in vitro and in vivo studies as well as divergent bacterial species. It is also possible that *S. aureus* biofilms may be recognized by alternative PRRs besides TLR2 or TLR9. For example, eDNA could also be sensed by other intracellular PRRs such as AIM2 or DNA-dependent activator of IFN regulatory factors (71, 72). The mechanism(s) responsible for TLR2/TLR9 evasion by *S. aureus* biofilms are not known but could also be explained by ligand inaccessibility. Indeed, our SEM data demonstrated that biofilms in vivo are encased within a complex three-dimensional structure with few free bacteria exposed at the outer surface (Fig. 2*B*), suggesting the inability to trigger PRRs expressed at the phagocyte surface. Alternatively, complex polysaccharide polymers that are known components of the biofilm matrix may interfere with

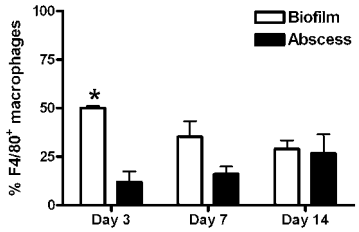

FIGURE 6. *S. aureus* biofilms elicit exaggerated macrophage infiltrates compared with abscesses. WT mice were infected with 5×10^5 CFU USA300 LAC::*lux* either in the lumen of surgically implanted catheters or s.c. in the absence of any indwelling device to establish biofilm and abscess infections, respectively. Animals were sacrificed at days 3, 7, or 14 following *S. aureus* exposure, whereupon tissues surrounding infected catheters or s.c. injection sites were collected to quantitate macrophage infiltrates by FACS. Results are expressed as the percent of $F4/80^+$ macrophages after correction for isotype control staining and represent the mean ± SEM of three independent experiments. Significant differences in macrophage infiltration into biofilm versus abscess infections are denoted by asterisks. $*p < 0.01$.

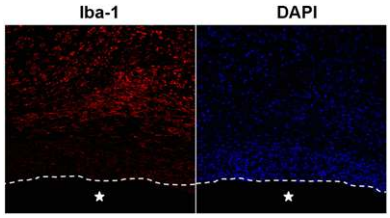

FIGURE 7. Macrophage migration toward *S. aureus* biofilms in vivo is limited. Tissues surrounding biofilm-infected catheters were collected from WT mice at day 7 following *S. aureus* infection and subjected to immunofluorescence staining with Iba-1 to identify macrophages (red) and DAPI to demarcate nuclei (blue) by confocal microscopy (original magnification ×20). Asterisks indicate the location of infected catheters, and the border between biofilm and surrounding host tissue is denoted by dashed lines. Results are representative of six individual animals.

optimal engagement of potential ligands with TLRs. However, these possibilities have yet to be investigated at the present time.

It is evident that *S. aureus* biofilms induce macrophage dysfunction at several levels, which provide potential explanations as to why these infections persist in an immunocompetent host. First, although biofilms induce greater macrophage influx during early infection compared with abscesses and harbor intracellular bacteria, the paucity of iNOS and robust arginase-1 expression suggest that bacteria may not be sufficiently cleared. A similar M2-like phenotype was observed in macrophages in vitro following biofilm coculture. Second, although biofilms were associated with robust macrophage accumulation, only a small subset of cells migrated toward the biofilm surface and many that expressed arginase-1, which skews macrophages for ineffective killing. Third, our findings clearly demonstrated that biofilms induced macrophage death by an as of yet unknown mechanism. Specifically, FACS staining with 7-AAD revealed significant macrophage cell death within 2 h following biofilm exposure. A longer coincubation period (i.e., 24 h) led to dystrophic macrophages with a ghostlike appearance, whereas cells cultured with 4-d-old biofilms demonstrated a typical shape even though a high percentage

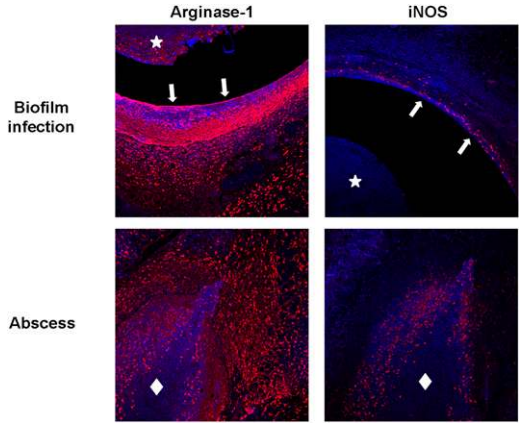

FIGURE 8. *S. aureus* biofilms repress iNOS and augment arginase-1 expression. WT mice were infected with 5×10^5 CFU USA300 LAC::*lux* either in the lumen of surgically implanted catheters or s.c. in the absence of any indwelling device to establish biofilm and abscess infections, respectively. Animals were sacrificed at day 7 following *S. aureus* exposure, whereupon tissues surrounding infected catheters or s.c. injection sites were collected and subjected to immunofluorescence staining with arginase-1 (red) and DAPI to identify nuclei (blue) by confocal microscopy (original magnification ×20). Stars represent the location of material remaining from the catheter lumen, and the diamonds denote the necrotic abscess core. The border between biofilm and surrounding host tissue is depicted by arrows. Results are representative of six individual animals.

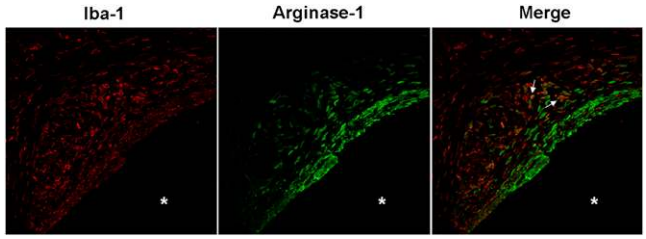

FIGURE 9. A subset of biofilm-associated macrophages expresses arginase-1. Tissues surrounding biofilm-infected catheters were collected from WT mice at day 7 following *S. aureus* infection and subjected to immunofluorescence staining for the macrophage-specific marker Iba-1 (red) and arginase-1 (green) to determine colocalization patterns by confocal microscopy (arrows, original magnification ×20). The position of the biofilm-infected catheter is denoted by asterisks. Results are representative of six individual animals.

of these macrophages were dead as revealed by TOTO3 staining. Importantly, macrophages were capable of phagocytizing bacteria from mechanically disrupted biofilms regardless of their maturation state, suggesting that the large size and/or inability to opsonize intact biofilms could explain the dystrophic macrophage phenotype. The latter possibility is supported by a recent study demonstrating that IgG and C3b deposition is reduced on the surface of biofilm-associated *S. epidermidis* compared with planktonic bacteria (16). Alternatively, PIA has antiphagocytic properties, which could also interfere with phagocytic uptake of *S. aureus* biofilms. It is important to note that the USA300 LAC strain used in the current study expresses PIA as demonstrated by WGA staining, but lacks a capsule (73); therefore, capsule cannot account for the antiphagocytic activity of the biofilm. The mechanism(s) that trigger macrophage cell death upon biofilm contact are not known but could be the result of acidic pH, bacterial toxins, and/or the hypoxic environment within the biofilm mass. Another question that remains is whether macrophage death following biofilm exposure is apoptotic or necrotic. Judging by the striking differences in macrophage morphology during incubation with immature versus mature biofilms, we speculate that both types of cell death are operative. Specifically, macrophages maintained their characteristic shape following extended (i.e., 24 h)

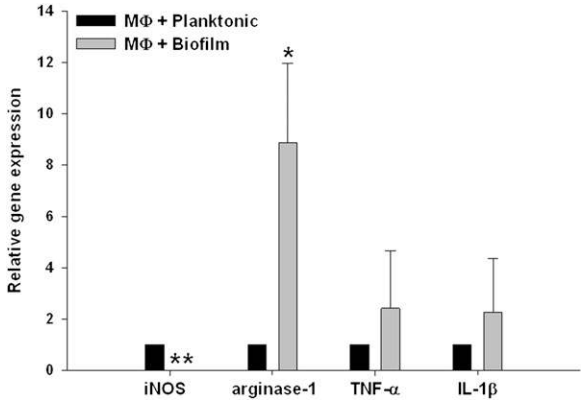

FIGURE 10. *S. aureus* biofilms skew macrophage gene expression toward an alternatively activated M2 phenotype. BMDM from GFP Tg mice were incubated with 6-d-old biofilms or planktonic bacteria for 2 h, whereupon viable macrophages were purified by FACS and RNA immediately isolated for qRT-PCR analysis. Gene expression levels in macrophages exposed to *S. aureus* biofilms were calculated after normalizing signals against GAPDH and are presented as the fold-change relative to macrophages incubated with planktonic bacteria. Results represent the mean ± SEM of four independent experiments. $*p < 0.05$, $**p < 0.001$.

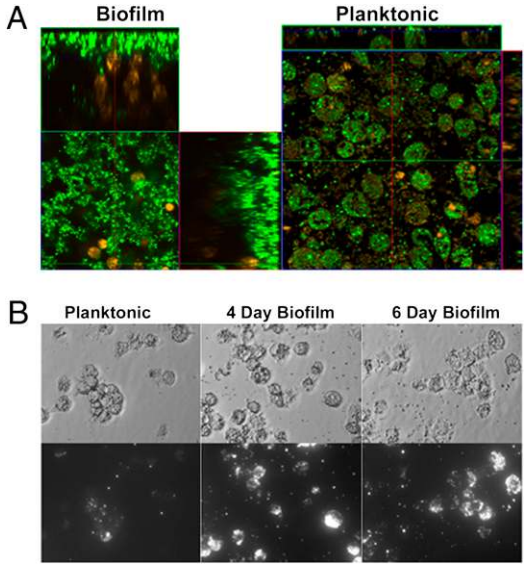

FIGURE 11. Macrophages actively phagocytize planktonic *S. aureus* but not biofilm-associated bacteria. *A*, Primary macrophages labeled with CTO (orange) were exposed to 4-d-old USA300 LAC-GFP biofilms or planktonic bacteria (green) for a 24-h period, whereupon visualization of intracellular bacteria was evaluated by confocal microscopy (original magnification ×63, 1 μm slice). Biofilm-associated macrophages exhibited little evidence of phagocytosis, whereas intracellular bacteria were readily detectable in macrophages incubated with planktonic organisms. Results are representative of six independent experiments. In *B*, 4- and 6-d-old USA300 LAC-GFP static biofilms were mechanically disrupted by triturating and incubated with macrophages for 1 h. Planktonic bacteria were included as a positive control. Fluorescent microscopy of cytospin preparations shows the ability of macrophages to phagocytize planktonic (*left panel*) as well as disassociated bacteria from 4- (*center panel*) and 6-d-old (*right panel*) biofilms. Results are representative of three independent experiments.

coculture with immature biofilms, whereas those macrophages that were exposed to mature biofilms for the same interval exhibited a wispy, dystrophic morphology reminiscent of necrotic cell death. Whether apoptosis and/or necrosis are responsible for macrophage death requires clarification in future studies.

Our results demonstrating that macrophages are capable of infiltrating biofilms are similar to previous reports using mixed leukocyte and purified neutrophil populations with *S. aureus*

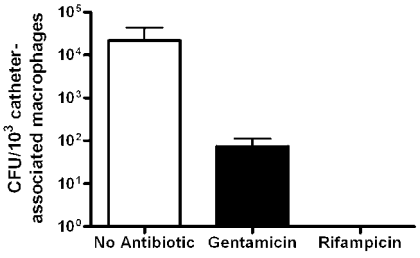

FIGURE 12. Macrophages recovered from *S. aureus* biofilm infections harbor viable intracellular bacteria. Viable macrophages ($F4/80^+$, 7-AAD^-) were recovered from tissues surrounding biofilm infections at day 7 postinfection by FACS, whereupon gentamicin protection assays were performed to evaluate the presence of viable intracellular bacteria. Controls included sorted macrophages without any antibiotic treatment (to assess extra- and intracellular bacteria) and macrophages treated with rifampicin, which is capable of penetrating the eukaryotic cell membrane. Results are expressed as the number of viable *S. aureus* (CFU per 10^3 biofilm-associated macrophages) and represent the mean ± SEM of five independent experiments.

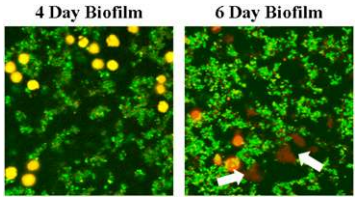

FIGURE 13. Macrophages exposed to mature *S. aureus* biofilm exhibit a dystrophic morphology. Primary macrophages labeled with CTO (yellow-orange) were exposed to 4- or 6-d-old USA300 LAC-GFP biofilms (green) for a 24-h period, whereupon visualization of macrophage morphology was evaluated by confocal microscopy (original magnification ×63, 1 μm slice). Macrophages infiltrating immature (4-d-old) biofilms retained a typical rounded morphology, whereas macrophages infiltrating mature biofilms (6-d-old) often exhibited a dystrophic ghostlike morphology with minimal retention of CTO (arrows). Results are representative of six independent experiments.

biofilms (17–19). However, several differences were also noted between these earlier studies and our own, including the fact that we did not observe appreciable phagocytosis of biofilm-associated *S. aureus* by macrophages in vitro, whereas studies with neutrophils reported bacterial uptake within the biofilm, which we also observed in the current report (Supplemental Fig. 4) (18, 19). In addition, other studies have reported that *S. aureus* biofilms elicit proinflammatory mediator release, which was not observed in our experiments. The reasons to account for these differences are not known but could be influenced by several factors including the method of biofilm propagation (i.e., static versus flow cell), the type of immune cell population examined, and/or compatibility of

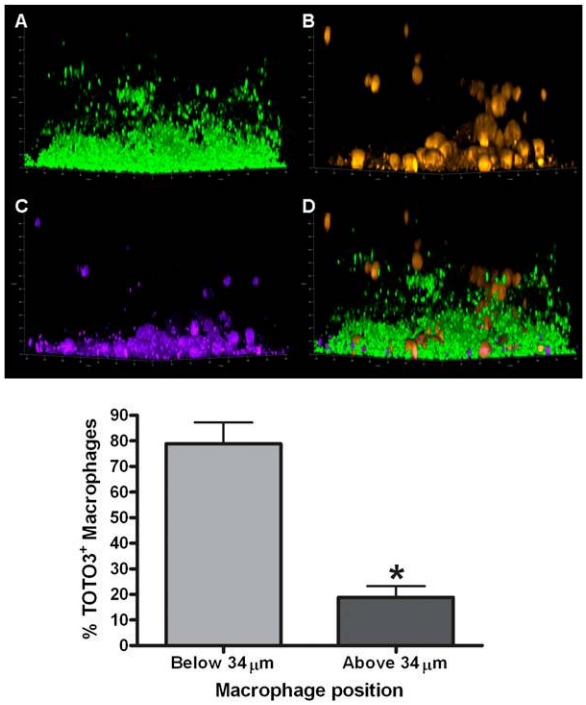

FIGURE 14. Macrophage viability is dictated by invasion into the biofilm proper. Four-day-old USA300 LAC-GFP biofilms (average height ~34 μm) (*A*) were incubated with primary macrophages labeled with CTO (*B*, yellow-orange) for a 24-h period, whereupon macrophage viability was determined by uptake of the live/dead stain TOTO3 (purple; *C*). The majority of dead ($TOTO3^+$) macrophages are within 34 μm of the biofilm proper ($p < 0.05$), and a composite image of all staining is shown (*D*). *Bottom panel,* Significant differences between the percentages of $TOTO3^+$ macrophages based on location within the biofilm proper are denoted with an asterisk. $*p < 0.05$; $n = 218$ cells.

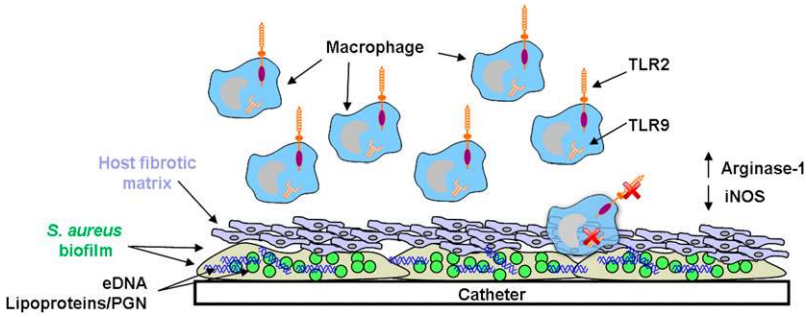

FIGURE 15. *S. aureus* biofilms skew macrophage responses to favor bacterial persistence. Despite the presence of TLR2 and TLR9 ligands within the biofilm (lipoproteins/PGN and eDNA, respectively), these traditional PRRs do not impart macrophage responsiveness or bacterial clearance during biofilm infection (depicted by red x marks). Likewise, the expression of iNOS is reduced following biofilm formation concomitant with an increase in arginase-1. Collectively, these changes shift the immune response away from a bactericidal pathway and likely contribute to biofilm persistence.

medium formulations to achieve optimal survival of both the biofilm and immune cells. Indeed, the dynamics of the flow system used in the previously cited studies could lead to less compact biofilms and enhanced bacterial detachment that would render *S. aureus* more susceptible to phagocytosis. Although in vitro experiments demonstrated minimal *S. aureus* phagocytosis, in vivo studies revealed that macrophages associated with *S. aureus* biofilms in vivo are capable of limited bacterial uptake. However, when taken in the context of minimal iNOS expression and adverse effects on cell viability, the ability of macrophages to efficiently kill intracellular *S. aureus* is likely compromised. In addition, because bacteria regularly detach from biofilms as part of their normal growth cycle to seed new sites of infection, it is possible that the intracellular bacteria detected in macrophages originated from the internalization of planktonic bacteria. Unfortunately, we are not able to discriminate between the uptake of biofilm-associated versus detached planktonic bacteria with any available technology. Nonetheless, our results collectively suggest that biofilms reprogram macrophage responsiveness toward a M2 phenotype that inherently possesses less antimicrobial activity (63, 64).

Another novel observation of the current study was the ability of *S. aureus* to establish a biofilm infection at a relatively low dose that was rapidly cleared following s.c. injection into sites lacking an indwelling device. The fact that fewer *S. aureus* are required to colonize foreign devices provides insights as to why indwelling devices are more prone to infection compared with natural body surfaces. It is likely that these artificial surfaces provide a niche for bacterial attachment either directly or indirectly when the foreign body becomes encased by host proteins that would facilitate the induction of biofilm growth. Collectively, these findings highlight the importance of studying indwelling device/biofilm-associated infections because of the blunted immune response and lower number of bacteria required to establish infection.

In summary, the current study demonstrates that *S. aureus* biofilms attenuate inflammatory mediator production and macrophage invasion into the biofilm. In addition, iNOS expression was attenuated, and a coincident increase in arginase-1 suggests a skewing of the immune response toward a profibrotic M2 phenotype. Another contributing factor is the ineffectiveness of classical TLR recognition pathways, which is likely dictated by the inability of tissue macrophages to significantly invade the biofilm proper in vivo. This result is in stark contrast with reports from other laboratories, demonstrating an important role of TLR2 and TLR9 in regulating planktonic *S. aureus* infection (74, 75). Therefore, it is evident that by assuming a biofilm growth state, *S. aureus* actively subverts the resultant host immune response, which likely contributes to biofilm persistence.

Acknowledgments

We thank Dr. Shizuo Akira for providing the TLR2 and TLR9 KO mice, Debbie Vidlak and Shuliang Liu for excellent technical assistance, Tom Bargar for performing SEM analysis, Fang Yu for statistical analysis, and Jennifer Endres for generation of the USA300 LAC::*lux* construct. We also thank Dr. Charles Kuszynski, Megan Michalak, and Victoria Smith in the UNMC Cell Analysis Facility for assistance with FACS analysis and the UNMC Tissue Science Facility for preparing paraffin sections.

Disclosures

The authors have no financial conflicts of interest.

References

1. Donlan, R. M., and J. W. Costerton. 2002. Biofilms: survival mechanisms of clinically relevant microorganisms. *Clin. Microbiol. Rev.* 15: 167–193.
2. Otto, M. 2008. Staphylococcal biofilms. *Curr. Top. Microbiol. Immunol.* 322: 207–228.
3. Fitzpatrick, F., H. Humphreys, and J. P. O'Gara. 2005. The genetics of staphylococcal biofilm formation—will a greater understanding of pathogenesis lead to better management of device-related infection? *Clin. Microbiol. Infect.* 11: 967–973.
4. Burlak, C., C. H. Hammer, M. A. Robinson, A. R. Whitney, M. J. McGavin, B. N. Kreiswirth, and F. R. Deleo. 2007. Global analysis of community-associated methicillin-resistant *Staphylococcus aureus* exoproteins reveals molecules produced in vitro and during infection. *Cell. Microbiol.* 9: 1172–1190.
5. Chambers, H. F., and F. R. Deleo. 2009. Waves of resistance: *Staphylococcus aureus* in the antibiotic era. *Nat. Rev. Microbiol.* 7: 629–641.
6. Voyich, J. M., K. R. Braughton, D. E. Sturdevant, A. R. Whitney, B. Saïd-Salim, S. F. Porcella, R. D. Long, D. W. Dorward, D. J. Gardner, B. N. Kreiswirth, et al. 2005. Insights into mechanisms used by *Staphylococcus aureus* to avoid destruction by human neutrophils. *J. Immunol.* 175: 3907–3919.
7. Takeuchi, O., K. Hoshino, and S. Akira. 2000. Cutting edge: TLR2-deficient and MyD88-deficient mice are highly susceptible to *Staphylococcus aureus* infection. *J. Immunol.* 165: 5392–5396.
8. Kobayashi, S. D., K. R. Braughton, A. R. Whitney, J. M. Voyich, T. G. Schwan, J. M. Musser, and F. R. DeLeo. 2003. Bacterial pathogens modulate an apoptosis differentiation program in human neutrophils. *Proc. Natl. Acad. Sci. USA* 100: 10948–10953.
9. Foster, T. J. 2005. Immune evasion by staphylococci. *Nat. Rev. Microbiol.* 3: 948–958.
10. Fournier, B., and D. J. Philpott. 2005. Recognition of *Staphylococcus aureus* by the innate immune system. *Clin. Microbiol. Rev.* 18: 521–540.
11. Walker, T. S., K. L. Tomlin, G. S. Worthen, K. R. Poch, J. G. Lieber, M. T. Saavedra, M. B. Fessler, K. C. Malcolm, M. L. Vasil, and J. A. Nick. 2005. Enhanced *Pseudomonas aeruginosa* biofilm development mediated by human neutrophils. *Infect. Immun.* 73: 3693–3701.
12. Mittal, R., S. Sharma, S. Chhibber, and K. Harjai. 2006. Effect of macrophage secretory products on elaboration of virulence factors by planktonic and biofilm cells of *Pseudomonas aeruginosa. Comp. Immunol. Microbiol. Infect. Dis.* 29: 12–26.
13. Chandra, J., T. S. McCormick, Y. Imamura, P. K. Mukherjee, and M. A. Ghannoum. 2007. Interaction of *Candida albicans* with adherent human peripheral blood mononuclear cells increases C. albicans biofilm formation and results in differential expression of pro- and anti-inflammatory cytokines. *Infect. Immun.* 75: 2612–2620.
14. Jensen, E. T., A. Kharazmi, K. Lam, J. W. Costerton, and N. Høiby. 1990. Human polymorphonuclear leukocyte response to *Pseudomonas aeruginosa* grown in biofilms. *Infect. Immun.* 58: 2383–2385.
15. Jesaitis, A. J., M. J. Franklin, D. Berglund, M. Sasaki, C. I. Lord, J. B. Bleazard, J. E. Duffy, H. Beyenal, and Z. Lewandowski. 2003. Compromised host defense on *Pseudomonas aeruginosa* biofilms: characterization of neutrophil and biofilm interactions. *J. Immunol.* 171: 4329–4339.
16. Kristian, S. A., T. A. Birkenstock, U. Sauder, D. Mack, F. Götz, and R. Landmann. 2008. Biofilm formation induces C3a release and protects *Staphylococcus* epidermidis from IgG and complement deposition and from neutrophil-dependent killing. *J. Infect. Dis.* 197: 1028–1035.

17. Leid, J. G., M. E. Shirtliff, J. W. Costerton, and P. Stoodley. 2002. Human leukocytes adhere to, penetrate, and respond to *Staphylococcus aureus* biofilms. *Infect. Immun.* 70: 6339–6345.
18. Günther, F., G. H. Wabnitz, P. Stroh, B. Prior, U. Obst, Y. Samstag, C. Wagner, and G. M. Hänsch. 2009. Host defence against *Staphylococcus aureus* biofilms infection: phagocytosis of biofilms by polymorphonuclear neutrophils (PMN). *Mol. Immunol.* 46: 1805–1813.
19. Guenther, F., P. Stroh, C. Wagner, U. Obst, and G. M. Hänsch. 2009. Phagocytosis of staphylococci biofilms by polymorphonuclear neutrophils: *S. aureus* and S. epidermidis differ with regard to their susceptibility towards the host defense. *Int. J. Artif. Organs* 32: 565–573.
20. Kobayashi, S. D., K. R. Braughton, A. M. Palazzolo-Ballance, A. D. Kennedy, E. Sampaio, E. Kristosturyan, A. R. Whitney, D. E. Sturdevant, D. W. Dorward, S. M. Holland, et al. 2010. Rapid neutrophil destruction following phagocytosis of *Staphylococcus aureus. J. Innate Immun.* 2: 560–575.
21. Graves, S. F., S. D. Kobayashi, and F. R. DeLeo. 2010. Community-associated methicillin-resistant *Staphylococcus aureus* immune evasion and virulence. *J. Mol. Med.* 88: 109–114.
22. Anwar, S., L. R. Prince, S. J. Foster, M. K. Whyte, and I. Sabroe. 2009. The rise and rise of *Staphylococcus aureus*: laughing in the face of granulocytes. *Clin. Exp. Immunol.* 157: 216–224.
23. Silva, M. T. 2010. Macrophage phagocytosis of neutrophils at inflammatory/infectious foci: a cooperative mechanism in the control of infection and infectious inflammation. *J. Leukoc. Biol.* DOI: 10.1189/jlb.0910536.
24. Silva, M. T. 2010. When two is better than one: macrophages and neutrophils work in concert in innate immunity as complementary and cooperative partners of a myeloid phagocyte system. *J. Leukoc. Biol.* 87: 93–106.
25. Rice, K. C., E. E. Mann, J. L. Endres, E. C. Weiss, J. E. Cassat, M. S. Smeltzer, and K. W. Bayles. 2007. The cidA murein hydrolase regulator contributes to DNA release and biofilm development in *Staphylococcus aureus. Proc. Natl. Acad. Sci. USA* 104: 8113–8118.
26. Whitchurch, C. B., T. Tolker-Nielsen, P. C. Ragas, and J. S. Mattick. 2002. Extracellular DNA required for bacterial biofilm formation. *Science* 295: 1487.
27. Allesen-Holm, M., K. B. Barken, L. Yang, M. Klausen, J. S. Webb, S. Kjelleberg, S. Molin, M. Givskov, and T. Tolker-Nielsen. 2006. A characterization of DNA release in *Pseudomonas aeruginosa* cultures and biofilms. *Mol. Microbiol.* 59: 1114–1128.
28. Mann, E. E., K. C. Rice, B. R. Boles, J. L. Endres, D. Ranjit, L. Chandramohan, L. H. Tsang, M. S. Smeltzer, A. R. Horswill, and K. W. Bayles. 2009. Modulation of eDNA release and degradation affects *Staphylococcus aureus* biofilm maturation. *PLoS ONE* 4: e5822.
29. Akira, S., S. Uematsu, and O. Takeuchi. 2006. Pathogen recognition and innate immunity. *Cell* 124: 783–801.
30. Hayashi, F., T. K. Means, and A. D. Luster. 2003. Toll-like receptors stimulate human neutrophil function. *Blood* 102: 2660–2669.
31. Bauer, S., C. J. Kirschning, H. Häcker, V. Redecke, S. Hausmann, S. Akira, H. Wagner, and G. B. Lipford. 2001. Human TLR9 confers responsiveness to bacterial DNA via species-specific CpG motif recognition. *Proc. Natl. Acad. Sci. USA* 98: 9237–9242.
32. Hertz, C. J., S. M. Kiertscher, P. J. Godowski, D. A. Bouis, M. V. Norgard, M. D. Roth, and R. L. Modlin. 2001. Microbial lipopeptides stimulate dendritic cell maturation via Toll-like receptor 2. *J. Immunol.* 166: 2444–2450.
33. Jones, B. W., T. K. Means, K. A. Heldwein, M. A. Keen, P. J. Hill, J. T. Belisle, and M. J. Fenton. 2001. Different Toll-like receptor agonists induce distinct macrophage responses. *J. Leukoc. Biol.* 69: 1036–1044.
34. Kirschning, C. J., and R. R. Schumann. 2002. TLR2: cellular sensor for microbial and endogenous molecular patterns. *Curr. Top. Microbiol. Immunol.* 270: 121–144.
35. Takeuchi, O., K. Hoshino, T. Kawai, H. Sanjo, H. Takada, T. Ogawa, K. Takeda, and S. Akira. 1999. Differential roles of TLR2 and TLR4 in recognition of gram-negative and gram-positive bacterial cell wall components. *Immunity* 11: 443–451.
36. Mercier, C., C. Durrieu, R. Briandet, E. Domakova, J. Tremblay, G. Buist, and S. Kulakauskas. 2002. Positive role of peptidoglycan breaks in lactococcal biofilm formation. *Mol. Microbiol.* 46: 235–243.
37. Cerca, N., K. K. Jefferson, R. Oliveira, G. B. Pier, and J. Azeredo. 2006. Comparative antibody-mediated phagocytosis of *Staphylococcus* epidermidis cells grown in a biofilm or in the planktonic state. *Infect. Immun.* 74: 4849–4855.
38. Moscoso, M., E. García, and R. López. 2006. Biofilm formation by *Streptococcus pneumoniae*: role of choline, extracellular DNA, and capsular polysaccharide in microbial accretion. *J. Bacteriol.* 188: 7785–7795.
39. Qin, Z., Y. Ou, L. Yang, Y. Zhu, T. Tolker-Nielsen, S. Molin, and D. Qu. 2007. Role of autolysin-mediated DNA release in biofilm formation of *Staphylococcus* epidermidis. *Microbiology* 153: 2083–2092.
40. Morath, S., A. Stadelmaier, A. Geyer, R. R. Schmidt, and T. Hartung. 2002. Synthetic lipoteichoic acid from *Staphylococcus aureus* is a potent stimulus of cytokine release. *J. Exp. Med.* 195: 1635–1640.
41. Weber, J. R., P. Moreillon, and E. I. Tuomanen. 2003. Innate sensors for Gram-positive bacteria. *Curr. Opin. Immunol.* 15: 408–415.
42. Dziarski, R. 2003. Recognition of bacterial peptidoglycan by the innate immune system. *Cell. Mol. Life Sci.* 60: 1793–1804.
43. Shimada, T., B. G. Park, A. J. Wolf, C. Brikos, H. S. Goodridge, C. A. Becker, C. N. Reyes, E. A. Miao, A. Aderem, F. Götz, et al. 2010. *Staphylococcus aureus* evades lysozyme-based peptidoglycan digestion that links phagocytosis, inflammasome activation, and IL-1beta secretion. *Cell Host Microbe* 7: 38–49.
44. Ip, W. K., A. Sokolovska, G. M. Charriere, L. Boyer, S. Dejardin, M. P. Cappillino, L. M. Yantosca, K. Takahashi, K. J. Moore, A. Lacy-Hulbert, and L. M. Stuart. 2010. Phagocytosis and phagosome acidification are required for pathogen processing and MyD88-dependent responses to *Staphylococcus aureus. J. Immunol.* 184: 7071–7081.
45. Hemmi, H., O. Takeuchi, T. Kawai, T. Kaisho, S. Sato, H. Sanjo, M. Matsumoto, K. Hoshino, H. Wagner, K. Takeda, and S. Akira. 2000. A Toll-like receptor recognizes bacterial DNA. *Nature* 408: 740–745.
46. Yoshimura, A., E. Lien, R. R. Ingalls, E. Tuomanen, R. Dziarski, and D. Golenbock. 1999. Cutting edge: recognition of Gram-positive bacterial cell wall components by the innate immune system occurs via Toll-like receptor 2. *J. Immunol.* 163: 1–5.
47. Watanabe, I., M. Ichiki, A. Shiratsuchi, and Y. Nakanishi. 2007. TLR2-mediated survival of *Staphylococcus aureus* in macrophages: a novel bacterial strategy against host innate immunity. *J. Immunol.* 178: 4917–4925.
48. Diep, B. A., A. M. Palazzolo-Ballance, P. Tattevin, L. Basuino, K. R. Braughton, A. R. Whitney, L. Chen, B. N. Kreiswirth, M. Otto, F. R. DeLeo, and H. F. Chambers. 2008. Contribution of Panton-Valentine leukocidin in community-associated methicillin-resistant *Staphylococcus aureus* pathogenesis. *PLoS ONE* 3: e3198.
49. Kennedy, A. D., M. Otto, K. R. Braughton, A. R. Whitney, L. Chen, B. Mathema, J. R. Mediavilla, K. A. Byrne, L. D. Parkins, F. C. Tenover, et al. 2008. Epidemic community-associated methicillin-resistant *Staphylococcus aureus*: recent clonal expansion and diversification. *Proc. Natl. Acad. Sci. USA* 105: 1327–1332.
50. Cassat, J. E., C. Y. Lee, and M. S. Smeltzer. 2007. Investigation of biofilm formation in clinical isolates of *Staphylococcus aureus. Methods Mol. Biol.* 391: 127–144.
51. Rupp, M. E., J. S. Ulphani, P. D. Fey, K. Bartscht, and D. Mack. 1999. Characterization of the importance of polysaccharide intercellular adhesin/hemagglutinin of *Staphylococcus* epidermidis in the pathogenesis of biomaterial-based infection in a mouse foreign body infection model. *Infect. Immun.* 67: 2627–2632.
52. Kielian, T., A. Cheung, and W. F. Hickey. 2001. Diminished virulence of an alpha-toxin mutant of *Staphylococcus aureus* in experimental brain abscesses. *Infect. Immun.* 69: 6902–6911.
53. Lauderdale, K. J., C. L. Malone, B. R. Boles, J. Morcuende, and A. R. Horswill. 2010. Biofilm dispersal of community-associated methicillin-resistant Staphylococcus aureus on orthopedic implant material. *J. Orthop. Res.* 28: 55–61.
54. Liu, S., and T. Kielian. 2009. Microglial activation by *Citrobacter* koseri is mediated by TLR4- and MyD88-dependent pathways. *J. Immunol.* 183: 5537–5547.
55. Thurlow, L. R., V. C. Thomas, S. D. Fleming, and L. E. Hancock. 2009. *Enterococcus faecalis* capsular polysaccharide serotypes C and D and their contributions to host innate immune evasion. *Infect. Immun.* 77: 5551–5557.
56. Drevets, D. A., and P. A. Campbell. 1991. Macrophage phagocytosis: use of fluorescence microscopy to distinguish between extracellular and intracellular bacteria. *J. Immunol. Methods* 142: 31–38.
57. Drevets, D. A., B. P. Canono, P. J. Leenen, and P. A. Campbell. 1994. Gentamicin kills intracellular *Listeria monocytogenes. Infect. Immun.* 62: 2222–2228.
58. Lauderdale, K. J., B. R. Boles, A. L. Cheung, and A. R. Horswill. 2009. Interconnections between Sigma B, agr, and proteolytic activity in *Staphylococcus aureus* biofilm maturation. *Infect. Immun.* 77: 1623–1635.
59. Kleinert, H., A. Pautz, K. Linker, and P. M. Schwarz. 2004. Regulation of the expression of inducible nitric oxide synthase. *Eur. J. Pharmacol.* 500: 255–266.
60. Curran, J. N., D. C. Winter, and D. Bouchier-Hayes. 2006. Biological fate and clinical implications of arginine metabolism in tissue healing. *Wound Repair Regen.* 14: 376–386.
61. Wynn, T. A. 2008. Cellular and molecular mechanisms of fibrosis. *J. Pathol.* 214: 199–210.
62. Hesse, M., M. Modolell, A. C. La Flamme, M. Schito, J. M. Fuentes, A. W. Cheever, E. J. Pearce, and T. A. Wynn. 2001. Differential regulation of nitric oxide synthase-2 and arginase-1 by type 1/type 2 cytokines in vivo: granulomatous pathology is shaped by the pattern of L-arginine metabolism. *J. Immunol.* 167: 6533–6544.
63. Gordon, S. 2003. Alternative activation of macrophages. *Nat. Rev. Immunol.* 3: 23–35.
64. Benoit, M., B. Desnues, and J. L. Mege. 2008. Macrophage polarization in bacterial infections. *J. Immunol.* 181: 3733–3739.
65. Boles, B. R., and A. R. Horswill. 2008. Agr-mediated dispersal of *Staphylococcus aureus* biofilms. *PLoS Pathog.* 4: e1000052.
66. Lauderdale, K. J., C. L. Malone, B. R. Boles, J. Morcuende, and A. R. Horswill. 2010. Biofilm dispersal of community-associated methicillin-resistant *Staphylococcus aureus* on orthopedic implant material. *J. Orthop. Res.* 28: 55–61.
67. Bainton, D. F., R. Takemura, P. E. Stenberg, and Z. Werb. 1989. Rapid fragmentation and reorganization of Golgi membranes during frustrated phagocytosis of immobile immune complexes by macrophages. *Am. J. Pathol.* 134: 15–26.
68. Fätkenheuer, G., O. Cornely, and H. Seifert. 2002. Clinical management of catheter-related infections. *Clin. Microbiol. Infect.* 8: 545–550.
69. Lowy, F. D. 1998. *Staphylococcus aureus* infections. *N. Engl. J. Med.* 339: 520–532.
70. Fuxman Bass, J. I., D. M. Russo, M. L. Gabelloni, J. R. Geffner, M. Giordano, M. Catalano, A. Zorreguieta, and A. S. Trevani. 2010. Extracellular DNA: a major proinflammatory component of *Pseudomonas aeruginosa* biofilms. *J. Immunol.* 184: 6386–6395.
71. Hornung, V., and E. Latz. 2010. Intracellular DNA recognition. *Nat. Rev. Immunol.* 10: 123–130.

72. Vilaysane, A., and D. A. Muruve. 2009. The innate immune response to DNA. *Semin. Immunol.* 21: 208–214.
73. Montgomery, C. P., S. Boyle-Vavra, P. V. Adem, J. C. Lee, A. N. Husain, J. Clasen, and R. S. Daum. 2008. Comparison of virulence in community-associated methicillin-resistant *Staphylococcus aureus* pulsotypes USA300 and USA400 in a rat model of pneumonia. *J. Infect. Dis.* 198: 561–570.
74. Takeuchi, O., K. Takeda, K. Hoshino, O. Adachi, T. Ogawa, and S. Akira. 2000. Cellular responses to bacterial cell wall components are mediated through MyD88-dependent signaling cascades. *Int. Immunol.* 12: 113–117.
75. Gillrie, M. R., L. Zbytnuik, E. McAvoy, R. Kapadia, K. Lee, C. C. Waterhouse, S. P. Davis, D. A. Muruve, P. Kubes, and M. Ho. 2010. Divergent roles of Toll-like receptor 2 in response to lipoteichoic acid and *Staphylococcus aureus* in vivo. *Eur. J. Immunol.* 40: 1639–1650.